Model Amphiphilic Block Copolymers with Tailored Molecular Weight and Composition in PDMS-Based Films to Limit Soft Biofouling

Brandon M. Wenning[1,2], Elisa Martinelli[2], Sophie Mieszkin[3], John A. Finlay[3], Daniel Fischer[4], James A. Callow[3], Maureen E. Callow[3], Amanda K. Leonardi[1], Christopher K. Ober[5], Giancarlo Galli[2]**

[1]Department of Chemistry and Chemical Biology, Cornell University, Ithaca, New York 14850

[2]Dipartimento di Chimica e Chimica Industriale, Università di Pisa, 56124 Pisa, Italy

[3]School of Biosciences, The University of Birmingham, Edgbaston, Birmingham B15 5TT, U.K.

[4]National Institute of Standards and Technology, Gaithersburg, Maryland 20899

[5]Department of Materials Science and Engineering, Cornell University, Ithaca, New York 14850

ABSTRACT: A set of controlled surface composition films was produced utilizing amphiphilic block copolymers dispersed in a crosslinked polydimethylsiloxane (PDMS) network. These block copolymers contained oligo(ethylene glycol) (PEGMA) and fluoroalkyl (AF6) side chains in selected ratios and molecular weights to control surface chemistry including antifouling and fouling-release performance. Such properties were assessed by carrying out assays using two algae, the green macroalga *Ulva linza* (favors attachment to polar surfaces) and the unicellular diatom *Navicula incerta* (favors attachment to non-polar surfaces). All films performed well against *U. linza* and exhibited high removal of attached sporelings (young plants) under an applied shear stress, with the lower molecular weight block copolymers being the best performing in the set. Composition ratios from 50:50 to 60:40 of the AF6:PEGMA side groups were shown to be more effective, with several films exhibiting spontaneous removal of the sporelings. Cells of *N. incerta* were also removed from several coating compositions. All films were characterized by surface techniques including captive bubble contact angle, atomic force

microscopy (AFM) and near edge X-ray absorption fine structure (NEXAFS) spectroscopy to correlate surface chemistry and morphology with biological performance.

KEYWORDS: *Antifouling, Fouling-Release, Block Copolymers, Fluoropolymers, Silicones, Ulva linza, Navicula incerta*

INTRODUCTION

Biofouling is caused by organisms and biomolecules settling and adhering to surfaces immersed in water. This process begins within minutes of immersion, and includes a wide range of fouling species.[1] Fouling of underwater surfaces, which includes the hulls of ships and immersed structures, significantly increases the operation and maintenance costs associated with loss of performance through drag and buildup of fouling organisms, which require removal[2,3]. For example, estimated biofouling costs for the US Navy, which only represents a small fraction of all ships, are $75–100M per year.[2] Internationally added fuel consumption to overcome decreased drag efficiency, contributes to significant production of greenhouse gasses.[4] Biocide-containing paints have been successful and are used extensively as antifouling coatings [5]. However some have been shown to be detrimental to the environment due to the effects of the biocides on non-target organisms and their persistence in waters and sediments.[6,7] As a result of these environmental concerns, biocidal coatings are becoming increasingly more regulated, creating a demand for high performance non-toxic alternatives.

Development of fouling-release (FR) and antifouling (AF) coatings requires a reduction in initial settlement (AF) or detachment of these organisms once attached (FR) by reducing their adhesion strength to the coatings. Non-toxic strategies which have been extensively investigated include the control of surface topology to affect the organisms' settlement behavior and adhesion

directly[8,9] as well as the use of bioactive molecules to act as chemical deterrents.[10–12] Chemical functionalities that have been introduced into AF coatings include polyions and zwitterions,[14–16] fluorocarbon side chains,[17] poly(ethylene glycol) (PEG) and fluorinated (macro)monomers in blends[18] and crosslinked networks,[19–21] as well as poly(ethylene glycol) (PEG).[22–24] Polydimethylsiloxane (PDMS) possesses an innate ability to release fouling organisms due to its low surface energy and Young's modulus.[25–28] Several strategies have been employed to improve the properties of PDMS coatings, including the addition of oils,[29] nanofillers,[30] antimicrobials,[31] amphiphilic oligopeptides[32] and surface-active polymers.[33–36] However, commercial coatings that employ some of these strategies accumulate microfouling[37,38] and may require grooming for optimum performance.[39]

Amphiphilic copolymers containing both polar and non-polar components[40] have been shown to act as AF materials. They incorporate protein resistance from hydrophilic groups such as PEG as well as surface directing low surface energy components such as alkyl, fluorinated, or siloxane groups.[34–36,41–46] Additionally, amphiphilic surfaces exhibit reconstruction underwater, making them responsive to the environment and promoting FR.[44,46–48]

In this work, we developed a range of surface-active amphiphilic PDMS-based block copolymers consisting of both PEG and fluoroalkyl side chain groups. Recent work utilized siloxane block copolymers with either a fluoroalkyl-containing or a PEG-containing block as additives to a PDMS network.[49] While this showed that fluoroalkyl and PEG chain groups acted independently, our goal was to ascertain whether combining these functionalities into one block copolymer could provide additional synergistic benefits of both groups in one film. It has been hypothesized that the combination of polar (PEG) and non-polar (fluoroalkyl/PDMS) units

creates an "ambiguous" surface, in which the fouling species encounters a surface that spontaneously alternates between polar and non-polar character.[50,51]

The PEG was incorporated as a hydrophilic component (PEGMA) to control the settlement of fouling organisms, a property which is widely known for PEG and the reason it is frequently used in AF applications.[44,51] The fluorinated component (AF6) was exploited as a surface-directing group for the block copolymer during film curing and furthermore it has been shown to be one of the few surface segregating species within a PDMS matrix, thus bringing both the fluoroalkyl segment and PEG to the coating surface.[52] The PDMS was incorporated in the block copolymer to enable compatibility with a PDMS matrix. The surface-active block copolymer was then blended into a PDMS matrix that was finally crosslinked, which provided the desired mechanical and surface energy properties to the films thereby promoting release of fouling organisms. The addition of amphiphilic components to a PDMS matrix has been investigated in applied studies,[33–36] but a detailed understanding of varying the ratio of fluoroalkyl and PEG containing groups on the surface chemistry of coatings does not yet exist. Prior studies have also not effectively determined the role of molecular weight of the block copolymer additives in controlling fouling release properties.

All surface-active block copolymers contained an identical PDMS block, onto which an ATRP initiator was attached. PEGMA and AF6 were copolymerized to form different sets of surface-active block copolymers with controlled and systematically varied molecular weight and hydrophilic and hydrophobic components. These block copolymers were then incorporated and locked into a crosslinked PDMS after directing the block copolymers to populate the coating surface. Biological assays were performed on the PDMS-based films containing different loadings of the surface-active block copolymers to assess the AF potential against two

widespread marine fouling organisms, the macroalga *Ulva linza*, and the diatom *Navicula incerta*. We were able to identify optimal composition ranges of the surface-active block copolymer additives based on these bioassays. Surface characterization data provided us with a better understanding of the trends which affect the AF and FR properties of these films. This in turn allowed us to design block copolymer additives for PDMS networks which are highly surface-active, producing multiple functionalities at the surface of the siloxane films.

EXPERIMENTAL SECTION

Materials. Tetrahydrofuran (THF), triethylamine (NEt_3), and dichloromethane (DCM) were distilled under nitrogen before use. Monocarbinol-terminated polydimethylsiloxane (Gelest) (M_n = 10000 g mol^{-1}, Si-OH), bissilanol-terminated polydimethylsiloxane (Gelest), (M_n = 26000 g mol^{-1}, PDMS), polydiethoxysiloxane (M_n = 134 g mol^{-1}, ES40) (Gelest), 2-bromo-isobutyryl bromide (BiBB) (Sigma-Aldrich, 98%), α,α,α-trifluorotoluene (TFT) (Aldrich, ≥99%), ethyl acetate (Aldrich), 1*H*,1*H*,2*H*,2*H*-perfluorooctyl acrylate (AF6) (Fluorochem, 97%), bismuth neodecanoate (BiND) (Sigma-Aldrich), poly(ethyleneglycol methyl ether methacrylate) (M_n = 300 g mol^{-1}, PEGMA) (Sigma-Aldrich), CuBr (Sigma-Aldrich, 99.9%) and N,N,N',N'',N''-pentamethyldiethylenetriamine (PMDETA) (Sigma-Aldrich, 99%) were used as provided.

Synthesis of Macroinitiator Si-Br. A single PDMS macroinitiator was prepared and used for block copolymerization (Figure 1). Details of the synthesis of this macroinitiator are given in Reference 49.

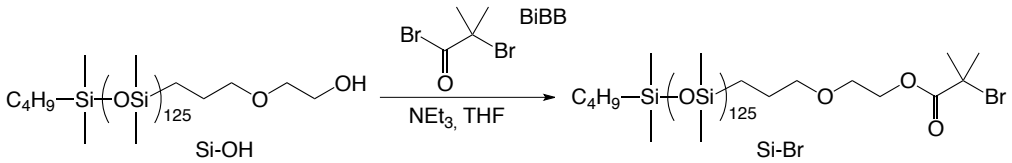

Figure 1. Schematic of macroinitiator synthesis for block copolymerization.

Copolymerization. All polymerizations were carried out by ATRP under the same conditions, only modifying the amount of the monomers AF6 and PEGMA added to each reaction to achieve different copolymers (Figure 2). Monomers were added at nine different ratios relative to each other and initiator concentration. The first set was targeted to produce copolymers using a mole comonomer to macroinitiator ratio of 30:1 added to the reaction, the second set at 60:1 and the third set at 150:1. The mole ratio between the monomers (AF6:PEGMA) for each set was 70:30, 50:50, and 30:70.

In a typical reaction the block copolymer L36, 1.2 g (0.12 mmol) of the macroinitiator Si-Br was added to a Schlenk tube along with 5.5 mL of TFT and 25 μL (0.12 mmol) of PMDETA. Afterwards 290 μL (1.08 mmol) of monomer AF6 and 720 μL (2.52 mmol) of monomer PEGMA were added. The mixture was freeze-pump-thawed 3 times and 17.2 mg (0.12 mmol) of CuBr was added to the reaction. The solution was freeze-pump-thawed 4 times, and finally heated to 115°C for 65 h under nitrogen. After the reaction was complete, DCM was added to the reaction solution. The solution was then washed 3 times with 5% $NaHCO_3$ and with deionized water 4 times until disappearance of blue-green color. The solution was dried with Na_2SO_4 and the DCM was removed using rotary evaporation. The polymer was then held under high vacuum for 18 h (yield 91%). The block copolymer had a M_n of 20 kg mol^{-1} and a mole ratio AF6:PEGMA of 36:64 and is denoted as L36. Related polymers have been previously reported in Reference 49, in which additional synthetic information is reported.

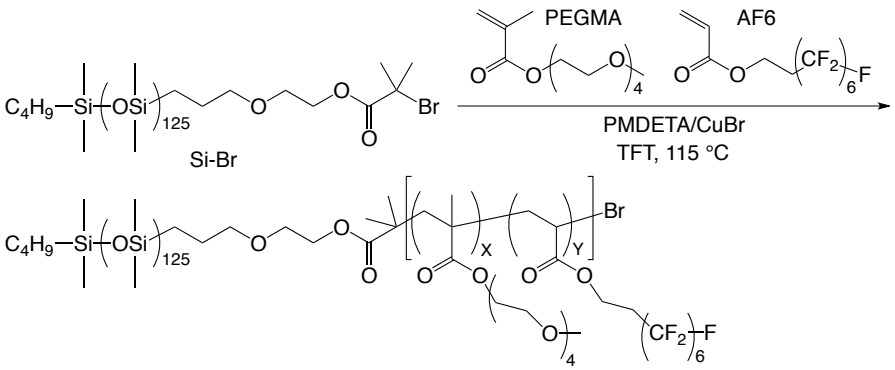

Figure 2. Schematic of ATRP block copolymerization of PEGMA and AF6 with formation of a copolymer block with varied composition (X and Y, respectively).

^{1}H NMR ($CDCl_3$): δ (ppm) = 0.1 ($SiCH_3$), 0.5 ($SiCH_2$), 0.9–2.6 ($CH_3CH_2CH_2$, CH_2CCH_3, $SiCH_2C\underline{H}_2$, $C(CH_3)_2$, CH_2CF_2, $CHCH_2$), 3.4–3.6 ($COOCH_2C\underline{H}_2(OC\underline{H}_2C\underline{H}_2)_3OC\underline{H}_3$, $COOCH_2C\underline{H}_2OC\underline{H}_2$), 4.1 ($COOC\underline{H}_2CH_2O$), 4.4 ($COOC\underline{H}_2CH_2CF_2$).

^{19}F NMR ($CDCl_3/CF_3COOH$): δ (ppm) = –6 (CF_3), –38 (CF_2CH_2), –45 to –49 (CF_2), –51 ($C\underline{F}_2CF_3$).

FT-IR (film): $\bar{\nu}$ (cm^{-1}) = 2962 (ν CH aliphatic), 1740 (ν C=O ester), 1400–1000 (ν $SiCH_3$, ν CO, ν SiO, ν CF), 803 (ν $SiCH_3$), 652 (ω CF_2).

Formation of PDMS Films. The PDMS was deposited in two steps onto acetone cleaned and dried glass slides (76 × 26 mm^2).

In a typical preparation of film L36:1, the matrix 5.0 g of PDMS, 0.125 g of crosslinker ES40 and 50 mg of catalyst BiND were dissolved in 25 mL of ethyl acetate. The solution was spray-coated using a Badger 250 airbrush. The films were dried at room temperature for 1 day and annealed at 120°C for a second day. A solution of the same composition, containing in addition 50 mg of the block copolymer 20/36:64 was cast on top of the first layer and cured at room temperature for 2 days and subsequently at 120°C for 1 day (overall thickness ca. 300 μm).

The surface-active block copolymers were added at loadings of 1 and 4 wt% concentrations as a fraction of the PDMS matrix. A blank PDMS film (i.e. without block copolymer) was used as a control.

Characterization. NMR spectra were made in $CDCl_3$ solution using a Varian Gemini 400MHz spectrometer. For ^{19}F NMR measurements, CF_3COOH was used as an internal reference. The ratio of AF6:PEGMA was determined by comparing peaks associated with the PEGMA units at 3.4–3.6 ppm and 4.1 ppm with those corresponding from the AF6 units at 4.4 ppm to determine relative compositions. In addition, the number average molecular weight M_n of the block copolymers were calculated from the observed peaks of the siloxane block at 0.1 and 0.5 ppm.

Molecular weight (M_n, M_w) and dispersity ($Đ$) of all polymers were determined (Table 1) using a Waters 1515 Isocratic HPLC pump ambient temperature chromatograph. The machine operating with THF solvent is equipped with both a Waters 2414 differential RI detector as well as a Waters 2489 UV/Visible detector. The GPC was calibrated using polystyrene standards.

Bubble Contact Angle. Water contact angle measurements were taken in triplicate with a Ramé-Hart model 100-00 NRL contact angle goniometer using deionized water at room temperature. The contact angle of an air bubble in contact with the surface underwater was determined using the captive bubble method previously described.[53] Specific details of this method are given in Reference 43.

NEXAFS. Near edge X-ray absorption fine structure (NEXAFS) experiments were carried out on the U7A NIST/Dow materials characterization end-station at the National Synchrotron Light Source (NSLS) at Brookhaven National Laboratory (BNL), the setup of which has been reported.[54] Experimental details have been reported elsewhere [41-44,55].

Samples were prepared the same way as for bioassays for analysis by NEXAFS. Samples were analyzed in both an as cast state and after immersion in deionized water for 72 h. Surfaces immersed in water were dried immediately before analysis and spectra were taken as quickly as possible to detect surface rearrangement in an aqueous environment.

Atomic force microscopy (AFM). All atomic force microscopy (AFM) experiments were performed using an MFP-3D-BIO system (Asylum Research Corp.) used in tapping mode. In the dry state, experiments were carried out in ambient conditions using silicon cantilevers with an Al-reflex coating, having a nominal force constant of 93 N m^{-1}, and a resonant frequency between 280 and 320 kHz, from AppNano (model: ACCESS-NC-A-W). In the wet state, experiments were carried out using the droplet method in deionized water, after being soaked for 7 days. Silicon nitride cantilevers with a gold tip-side coating and a gold/chromium reflex coating were used, with a nominal force constant of 0.09 N m^{-1} and a resonant frequency of between 8 and 10 kHz in water, from Olympus (model: OMCL-TR400PB). Surface roughness was calculated over areas of 5 x 5 μm.

Laboratory Bioassays.

Assays with N. incerta. For the assays with the diatom *Navicula*, 6 slides were equilibrated in artificial seawater (ASW; Tropic Marin) for 72 h prior to use. A suspension of diatom cells cultured in F/2 medium was filtered through 50 and 20 μm nylon meshes and then adjusted to give a chlorophyll content of 0.25 μg mL^{-1}. 10 mL of the diatom suspension were added to each slide placed into individual compartments of polystyrene 4-compartments plates (quadriPERM® dishes, Greiner Bio-One Ltd). After 2 h at ambient (ca. 20°C) all slides were washed with filtered ASW to eliminate unsettled (unattached) cells from the surface. At this

time, three of the slides were fixed using 10 mL 2.5% (v/v) glutaraldehyde in ASW and then rinsed in deionised water before air-drying overnight. Attached cells were counted by chlorophyll autofluorescence using AxioVision 4 image analysis system attached to a Zeiss epifluorescent microscope (20× objective; λ excitation and emission: 546 and 590 nm, respectively). A total of 30 fields of view were counted for each replicate slide (each 0.15 mm^2). The mean count (n=90) was then converted to number per mm^2.

The other three slides after rinsing with ASW were put directly into a calibrated turbulent flow channel previously described[56] to test the adhesion strength of the diatom cells. Water in turbulent flow with a wall shear stress of 56 Pa was flowed across the slides for 5 min. Again, the cells were fixed using glutaraldehyde. The number of remaining cells was counted and was compared to the unexposed slides to evaluate the fraction of cells removed.

Zoospores and sporelings of U. linza. For assays with *U. linza*, 9 slides were equilibrated in filtered ASW for 72 h prior to the assays. Motile zoospores were released into ASW from mature plants using a standard method,[57] then diluted in 0.22 μm filtered ASW to obtain an a suspension containing approximately 1×10^6 spores mL^{-1}. 10 mL of spore suspension were added to each slide placed in an individual compartment of quadriPERM® dishes, and the spores were allowed to settle in complete darkness for 45 minutes. After that time, all slides were rinsed gently using filtered ASW. Three of the slides for each polymer were fixed and quantified as described previously for cells of *N*. incerta. The remaining 6 slides, were rinsed in ASW before placing in individual compartments of quadriPERM® dishes, and 10 mL enriched seawater medium. The slides were incubated at 18 °C with a 16h:8h light:dark cycle and with a light intensity of 40 μmol m^{-2} s^{-2} for 7 days to allow the growth of the sporelings on the films. After the first 24 h and then every 2 days the medium was refreshed. The biomass of sporelings on the

surfaces was determined by quantifying the fluorescence of chlorophyll using a plate reader (TECAN, GENios Plus) in relative fluorescence units (RFU) as previously described.[58]

To evaluate the ease of removal of sporelings, these 6 slides were then exposed for 5 min to a wall shear stress of 8 Pa in a calibrated water channel. Biomass remaining after flow on the surfaces was again determined using a plate reader and was compared to unexposed samples to determine the percentage of sporelings removed.

Statistical analyses. Differences between settlement densities of spores/cells and biomass of sporelings were tested using one-way ANOVA followed by Tukey's test for pairwise comparisons using the software Minitab 15 as the data conformed to normality assumptions. Significant differences showed $p<0.05$. The percentage removal of spores/cells and sporelings was calculated from readings taken before and after exposure to flow, with 95% confidence limits calculated from arcsine-transformed data. Differences between surfaces were evaluated as previously described.

RESULTS

Physicochemical Characterization. In order to carry out our studies, we prepared a systematic series of polymers with a selection of physical characteristics. All the block copolymers were prepared by ATRP from a mixture of the poly(ethylene glycol methyl ether methacrylate) (PEGMA) and 1*H*,1*H*,2*H*,2*H*-perfluorooctyl acrylate (AF6), starting from a bromine-terminated PDMS macroinitiator (Si-Br, M_n = 10000 g mol^{-1}) (Figures 1 and 2). It was possible to synthesize three sets of block copolymers, with different lengths of the second block, by changing the monomer/macroinitiator feed mole ratio (from 30:1 to 150:1), while keeping the reaction time constant (66 h) (Table 1). Overall therefore 9 surface-active compositions were

produced for testing. The hydrophobic/hydrophilic balance of the resulting block copolymers was adjusted by regularly varying the AF6:PEGMA initial feed mole ratio (from 70:30 to 30:70) (Table 1). There were small differences between the AF6:PEGMA mole ratio in the comonomer initial feed and the final block copolymer composition that became comparatively large at the highest AF6:PEGMA feed mole ratio of 70:30. Therefore, the controlled modulation of the adopted synthetic scheme enabled preparation of block copolymers with controlled and targeted chemical, amphiphilic character. We have observed that the overall composition and the relative molecular weight are important factors in their antifouling characteristics. Copolymers listed in Table 1 are therefore identified by a shorthand name including either L, M, or H corresponding to low, medium, or high overall molecular weight respectively, based on the 30:1, 60:1, and 150:1 comonomer:macroinitiator composition ratios. The low molecular weight diblocks (L) range from 19 to 24 kg mol^{-1}, the medium molecular weight diblocks (M) range from 28 to 31 kg mol^{-1} and the high molecular weight diblocks (H) range from 54 to 65 kg mol^{-1}. The composition in the final polymer changed slightly from the reaction mixture, therefore we used the ratio of the two blocks experimentally determined for the final product for the sample name. The number thus corresponds to the measured mole percentage of AF6 in the diblock copolymer, which implies the PEGMA content is the remaining percentage not listed in the shorthand name. For example, L36 is one of the low molecular weight diblock copolymers made from the macroinitiator and a low amount of monomer using a 30:70 AF6:PEGMA mixture. Other polymers are named similarly.

To create AF/FR films the block copolymers were dispersed in a PDMS matrix at different loadings as surface-active components.

Table 1. Polymerization Conditions and Physicochemical Characterization of the Block Copolymers.

	Monomer:macroinitiator [a] 30:1			Monomer:macroinitiator [a] 60:1			Monomer:macroinitiator [a] 150:1		
Block copolymer	L36	L48	L59	M29	M51	M61	H25	H48	H62
AF6 [b]	1.08	1.80	2.52	2.16	3.60	5.04	5.40	9.00	12.60
PEGMA [b]	2.52	1.80	1.08	5.04	3.60	2.16	12.60	9.00	5.40
AF6:PEGMA [c]	30:70	50:50	70:30	30:70	50:50	70:30	30:70	50:50	70:30
$M_{n,GPC}$ ($Đ$) [d]	20 (1.16)	19 (1.14)	18 (1.16)	25 (1.34)	22 (1.21)	21 (1.12)	33 (1.65)	31 (1.45)	30 (1.35)
$M_{n,NMR}$ [e]	19	23	24	20	30	31	65	56	54
AF6:PEGMA [f]	36:64	48:52	59:41	29:71	51:49	61:39	25:75	48:52	62:38

[a] Comonomer (AF6+PEGMA):macroinitiator mole ratio in the initial feed.
[b] Amount (in mmol) of monomers in the initial feed.
[c] Mole ratio of monomers in the initial feed.
[d] GPC number average molecular weight (in kg mol^{-1}) and dispersity.
[e] Molecular weight calculated from NMR (in kg mol^{-1})
[f] Mole ratio of repeat units in the block of block copolymer.

Preparation of PDMS-Based Films. For the preparation of the blend films, a standard two step procedure was followed [34]. In the first step, a solution of the bis(silanol)-terminated PDMS, ES40 crosslinker and BiND catalyst was spray-coated on glass slides and cured at room temperature for 24 h and at 120°C for 24 h to form a primer layer. The block copolymers were blended at different loadings (1 and 4 wt%) with respect to the PDMS matrix. Films are identified by the block copolymer blended into the PDMS matrix as shown in Table 1 with the loading percentage listed after, for example L36:1 means polymer L36 added to the PDMS matrix at 1 wt%.

Laboratory Bioassays. Use of green macroalga *U. linza*, and the unicellular slime forming alga (diatom) *N. incerta* provide the ability with two fouling organisms to test fouling preferential for polar (*U. linza*) and non-polar (*N. incerta*) surfaces. Only three films (M29:1, M29:4 and H25:1) had significantly lower spore settlement than the PDMS control (i.e. with no block copolymer additive), and one (H25:4) had the same level of settled spores as the PDMS

control (Figure 3). All of these films derived from the 30:70 AF6:PEGMA feed ratio from both the 60:1 and 150:1 monomer:macroinitiator compositions (Figure 3b) containing relatively high amounts of PEGMA. The remaining films had significantly higher settlement densities than the PDMS control. Different values for spore settlement on PDMS were found in the two batch assays owing to inherent biological variability of separate spore preparations, even though all released from parent material collected in the wild.

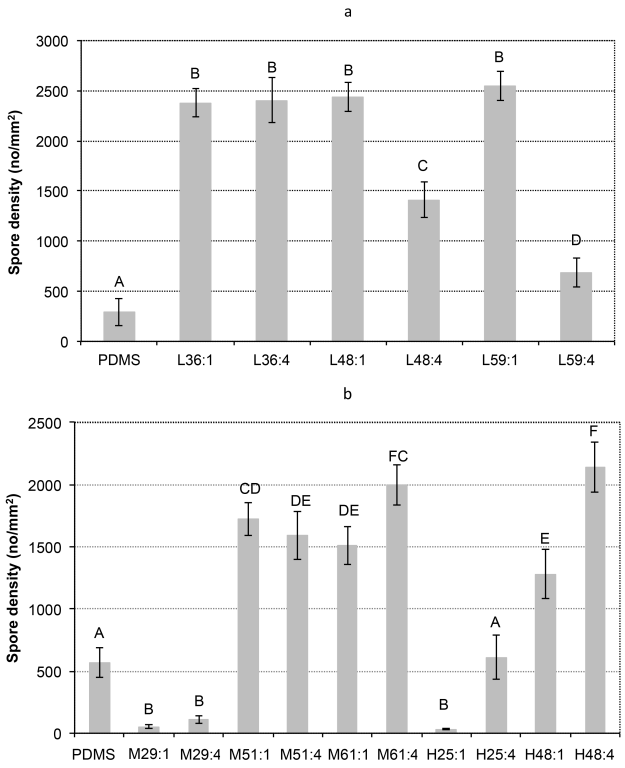

Figure 3. Effect of PDMS and amphiphilic PDMS-based surfaces in batch (a) L36:1 to L59:4 (Low, 19–24 kg mol^{-1}) and batch (b) M29:1 to M61:4 (Medium, 28–31 kg mol^{-1}) and H25:1 to H48:4 (High, 56–65 kg mol^{-1}) on the settlement of spores of *U. linza*. Mean density of settled spores was obtained from the count of three replicate slides (n=90). Error bars represent ± 2 × SE. Values that are significantly different to each other at $p<0.05$ are indicated by different letters. Surfaces were assayed in two batches, with two separate spore preparations, all released from parent material collected in the wild.

After culturing spores of *Ulva* to the stage of sporelings, (i.e. small plants), the biomass present on each film was measured indirectly as relative fluorescence units (RFU) (Figure 4). The density of sporelings broadly reflected spore settlement as described above. It was noted that sporeling biomass on the L36:4 and L48:4 films after 7 days growth was decreased due to spontaneous detachment of the sporelings induced by gentle movement of the dishes during replenishment of nutrient solution (Figure 4a). This highlights the low attachment strength of *Ulva* sporelings to these films even without the application of shear provided by a flow channel.

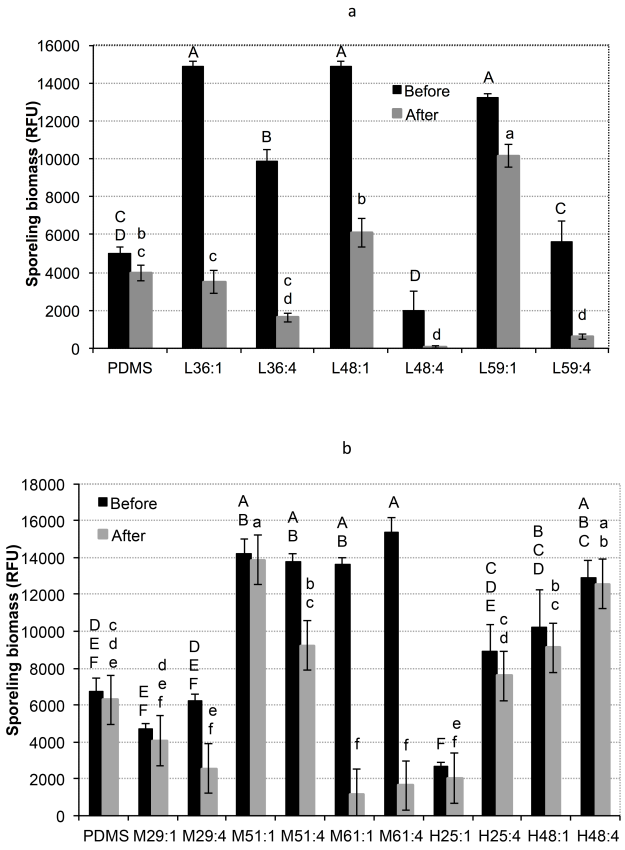

Figure 4. Effectiveness of PDMS and amphiphilic PDMS-based surfaces in batch (a) L36:1 to L59:4 (Low, 19–24 kg mol^{-1}) and batch (b) M29:1 to M61:4 (Medium, 28–31 kg mol^{-1}) and H25:1 to H48:4 (High, 56–65 kg mol^{-1}) on the biomass sporelings of *U. linza* before and after 5 min exposure to 8 Pa shear stress. Error bars represent ± SE. Values that are significantly different to each other at $p<0.05$ are indicated by different letters (uppercase before shear, lower case after shear).

Strength of attachment assays (expressed as % removal) indicated that many of the films possessed good FR properties with several showing nearly complete removal after being subject to a relatively low shear stress (8 Pa) (Figure 5). In general, films with 4 wt% of block copolymer performed better, or as well as, those with only 1 wt%. However, this trend was not apparent for the highest molecular weight block copolymers, for which significant differences were not revealed. Additionally, the lower molecular weight block copolymers showed better performance than those of highest molecular weights.

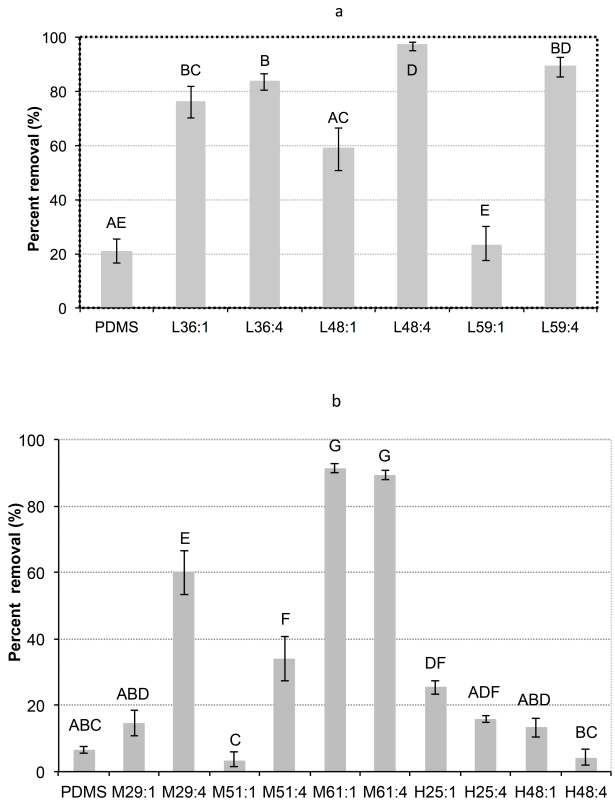

Figure 5. Effectiveness of PDMS and amphiphilic PDMS-based surfaces in batch (a) L36:1 to L59:4 (Low, 19–24 kg mol^{-1}) and batch (b) M29:1 to M61:4 (Medium, 28–31 kg mol^{-1}) and H25:1 to H48:4 (High, 56–65 kg mol^{-1}) on the attachment strength of *U. linza* sporelings. Mean percentage removal of sporelings after 5 min exposure to a shear stress of 8 Pa obtained from RFU measurements on 6 replicate slides prior to and after exposure to flow. Error bars represent ± SE, calculated from arcsine-transformed data. Values that are significantly different to each other at $p<0.05$ are indicated by different letters.

Based on the excellent FR properties of the films L36:1 through L59:4 with lowest molecular weight block copolymer additives, these samples were then also tested for their performance against *N. incerta*, a diatom (Figure 6). Diatoms show very different settlement characteristics compared to *U. linza*, typically adhering strongly to hydrophobic surfaces such as PDMS.[59,60] Diatoms cannot actively select the surfaces for attachment since they are not motile in the water column. Cells reach the surface by gravity in the case of laboratory assays, or through transport in water currents in the natural environment. The initial attachment density of diatoms provides a measure of the coatings' ability to resist adhesion on the surface. Films L48:4 and L59:4 had the lowest initial attachment and had a significantly lower number of attached cells (400 per mm^2) compared to the PDMS control (600 per mm^2) (Figure 6a). Overall, the attachment strength of cells of *N. incerta* on the block copolymer films was noticeable, with the films matching the PDMS control. Removal was greatest from the 48:52 AF6:PEGMA (L48:1 and L48:4) films at 32 and 29%, respectively (Figure 6b). Our findings suggest that the characteristics of the films showed improvement in inhibiting attachment of diatoms but not as fouling-release coatings.

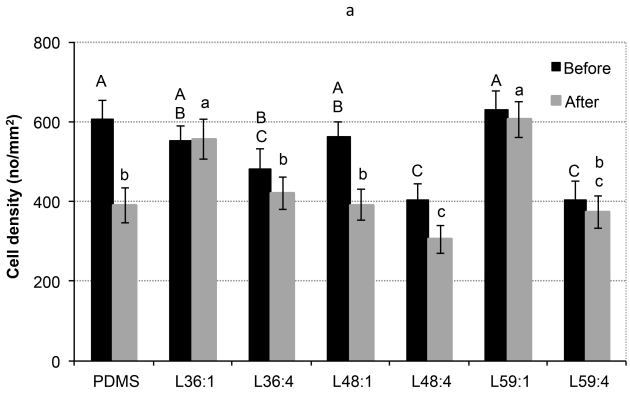

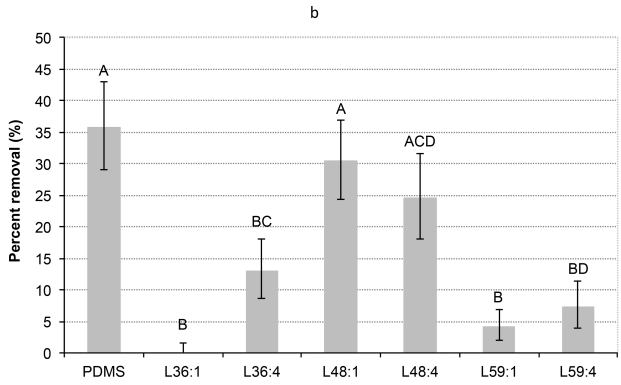

Figure 6. Effectiveness of PDMS and amphiphilic PDMS-based surfaces L36:1 to L59:4 (Low, 19–24 kg mol^{-1}) on initial attachment and adhesion strength of cells of *N. incerta*. (a) Mean density of settled cells obtained from the count of three replicate slides (n=90). Error bars represent ± 2 × SE. (b) Mean percentage removal of cells calculated from the counts of three replicate slides after 5 min exposure to 56 Pa shear stress. Error bars represent ± 2 × SE, calculated from arcsine-transformed data. Values that are significantly different to each other at $p<0.05$ are indicated by different letters (uppercase before shear, lower case after shear).

Bubble contact angle measurements on PDMS-based films. Bubble contact angle measurements were taken immediately after immersion of the surfaces in water, and at different times (t = 0, 12, 24, 48, 72, 96, and 120 h) after the initial immersion to study time-dependent surface wettability after exposure to water (Table 2). A time-dependent behavior is related to rearrangement of the surface chemical groups upon immersion in water, and shows the dynamic nature of these surfaces.

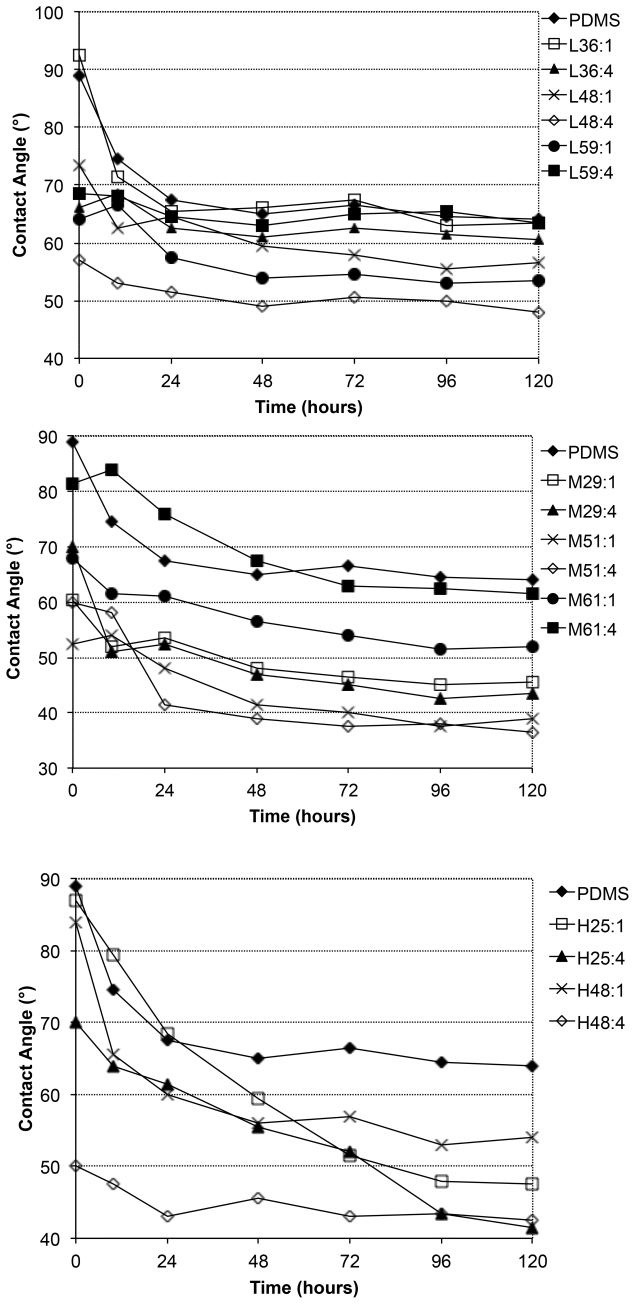

Figure 7. Bubble contact angle measurements taken under water over 120 h of immersion in deionized water. PDMS-based films are grouped by length of surface-active block copolymer. Plots are divided by molecular weight range of the block copolymer additives, showing (top) L36:1 to L59:4 (Low, 19–24 kg mol^{-1}), (middle) M29:1 to M61:4 (Medium, 28–31 kg mol^{-1}), and (bottom) H25:1 to H48:4 (High, 56–65 kg mol^{-1}).

Table 2. Bubble Contact Angle Measurements (in Degrees) Taken Under Water by Captive Bubble After 120 h Immersion in Deionized Water

Sample	Contact Angle	Sample	Contact Angle	Sample	Contact Angle
L36:1	64±3	M29:1	46±2	H25:1	48±3
L36:4	61±4	M29:4	44±3	H25:4	42±3
L48:1	57±2	M51:1	39±2	H48:1	54±2
L48:4	48±2	M51:4	37±2	H48:4	43±3
L59:1	54±4	M61:1	52±3		
L59:4	64±3	M61:4	62±3	PDMS	64±2

For all samples the bubble contact angle decreased after continued immersion in water, with most samples reaching equilibrium within 24–48 h of immersion as can be seen in Figure 7. Generally, the addition of all the amphiphilic PDMS-based block copolymers made the surfaces more hydrophilic, depressing the initial contact angle measurements (t = 0) down to values lower (e.g., 50° for H48:4) than that of PDMS (89°). After 120 h, the submerged contact angles of the films containing the higher molecular weight block copolymers M and H were generally much lower than those with the lowest molecular weight additive. This trend correlates with the total content of PEGMA in the films, as the higher molecular weight additives contained a higher percentage of the PEGMA relative to their molecular weight. For each of the sets of samples with similar molecular weights, the samples with a nearly 50:50 AF6:PEGMA ratio showed the lowest contact angle values at t = 120 h.

NEXAFS and AFM Studies of PDMS-based films. To understand the surface chemistry of these films and how it relates to their biological performance, the final surfaces were characterized by NEXAFS and AFM analyses to explore the effect of block copolymer content and composition on surface chemistry of the films. Comparing features observed in previously successful films, namely relative populations of components of the amphiphilic block copolymers, orientation of selected groups, and differences in films prior to and after immersion

in water can give insight into surface chemical features which help to design films with improved AF/FR effectiveness.

For the NEXAFS spectra of these samples (Figure 8a), the peak at 289.5 eV is associated with the $1s \rightarrow \pi^*_{C=O}$ resonance from the ester of the AF6 acrylate and PEGMA methacrylate groups along with the peak at 300 eV due to an additional C=O resonance. A distinct peak at 288 eV can be assigned to a $1s \rightarrow \sigma^*_{C-H}$ resonance while a broad peak at 291 eV is due to the $1s \rightarrow \sigma^*_{C-Si}$ resonance of PDMS. The σ^*_{C-F} and σ^*_{C-C} resonances, both due to the the fluoroalkyl segment, result in signals at 294 eV and 299 eV, respectively.

The σ^*_{C-F} peak possessed a significant angular dependence, indicating orientation of the segments perpendicular to the surface. The increasing intensity of the peak with increasing angle θ indicates that the orientation of the C–F bond was perpendicular to the surface normal (Figure 8b) and thus the fluoroalkyl segments were oriented normal to the surface, surprising given its relatively low concentration and the competition with both PDMS and PEG for surface dominance.

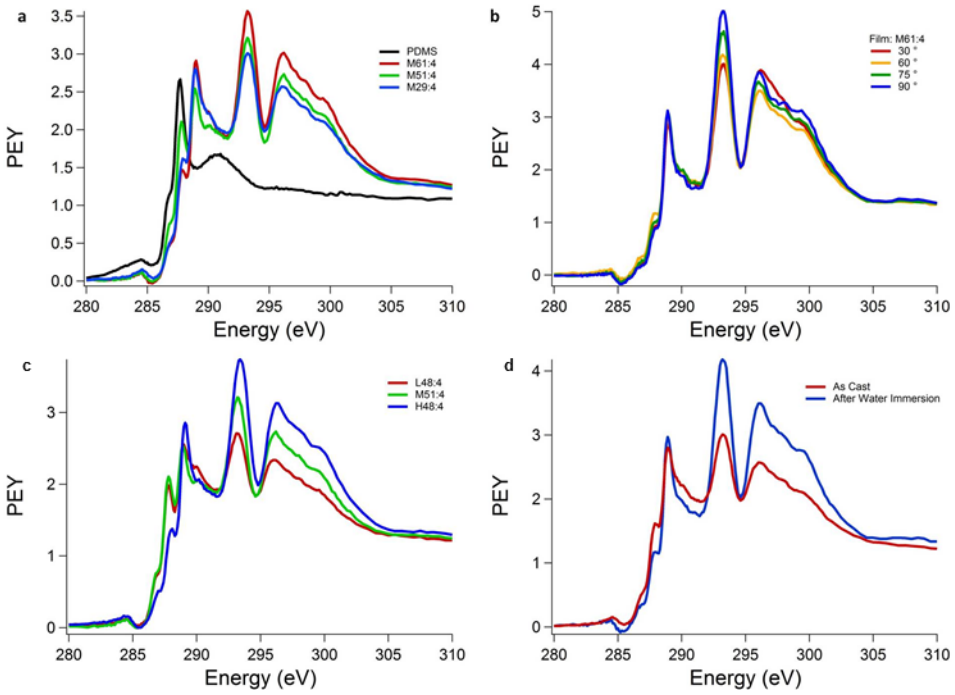

Figure 8. (a) NEXAFS spectra (θ = 51°) comparing films of PDMS, M29:4, M51:4, and M61:4 showing the effects of block copolymer composition on surface chemistry. (b) Overlap of NEXAFS spectra taken at varying experimental angle, θ, for film M61:4 showing angle dependence of emission spectra. (c) NEXAFS spectra (θ = 55°) comparing films of L48:4, M51:4, and H48:4 showing the effects of block copolymer molecular weight on surface chemistry. (d) NEXAFS spectra of film M61:4 (θ = 55°) prior to and after immersion in deionized water for 72 h showing reconstruction of the film surfaces.

Comparisons of spectra from different samples also give information about how block copolymer chemistry can affect relative surface composition for each film (Figures 8a and 8c). Comparison of the control PDMS with M29:4, M51:4, and M61:4 shows how varying chemical composition of the block copolymer affected surface chemistry (Figure 8a). These three films contain block copolymers with similar molecular weights, and varying compositions of AF6:PEGMA. Increasing the AF6 content of the block copolymer enriched the surface in fluorinated components while decreasing the silicone content at the surface. Importantly, however, this delivered the PEGMA to the near surface region and indicates that it is possible to control surface composition with these block copolymers.

Comparison of NEXAFS spectra taken of films with different block copolymer molecular weights but similar composition in Figure 8c shows how the surface chemistry is varied by block copolymer molecular weight. As the molecular weight was increased, the relative surface content of the siloxane block was decreased, while the fluoroalkyl and PEG content was increased. This effect is likely based on the fact that the higher molecular weight additives have a higher fraction of the PEG and fluoroalkyl groups relative to the siloxane block.

Additionally, comparing the spectra of M61:4 before and after a 72 h immersion in deionized water gives insights into the underwater surface rearrangement for these surfaces (Figure 8d). After immersion, both the carbonyl and fluoroalkyl peaks increased while the peak associated with PDMS decreased, consistent with a reconstruction of the film surface that drives both AF6 and PEGMA units to the polymer–water interface. Recent XPS studies[47] on amphiphilic block copolymers containing a poly(fluorostyrene) block carrying PEG side chains demonstrated that the low surface energy fluorinated units segregated to the air-polymer interface that occurred during film formation also resulted in an effective transport of the hydrophilic oxyethylenic side chains to the film surface. Consequently, the PEG segments could promptly expand outwards after being immersed in water to increase their contact with the external environment and enrich the film surface. The changes in the NEXAFS spectra show that when immersed in water the present block copolymers also surface segregated and populated the surface of the films. For these block copolymers to control performance of the films underwater, they need to surface segregate in aqueous environments. Thus, NEXAFS studies show that not only do the block copolymers remain surface-active underwater, but they are significantly enriched at the surface. This observation correlates with the bubble contact angle measurements, which exhibited increased hydrophilicity underwater with time, based on reconstruction of the

film surfaces. Additionally, these block copolymers must surface segregate underwater owing to the PEGMA populating the near surface region. While NEXAFS shows that this effect drives surface segregation strongly underwater, contact angle measurements suggest that it can be fine tuned based on the block copolymer chemistry employed.

AFM analysis revealed two distinct morphologies among coatings, represented by L48:1 and L48:4 in Figure 9. L48:1, which has a lower loading of AF6:PEGMA copolymer, showed small nodule structures ranging from 300 to 500 nm in diameter, with a measured root-mean-square (RMS) surface roughness of 17.6 nm. In contrast, the higher loaded L48:4 had a RMS surface roughness of 1.8 nm and formed a relatively featureless surface. Immersion in deionized water for 7 days did not result in any significant changes to the surface morphology in either sample, but in both cases an increase in surface roughness was observed, to 22.1 and 3.0 nm, respectively. In general, higher loadings of AF6:PEGMA led to smoother, more homogenous surfaces, which can be further seen in Figures S1 and S2 in Supporting Information.

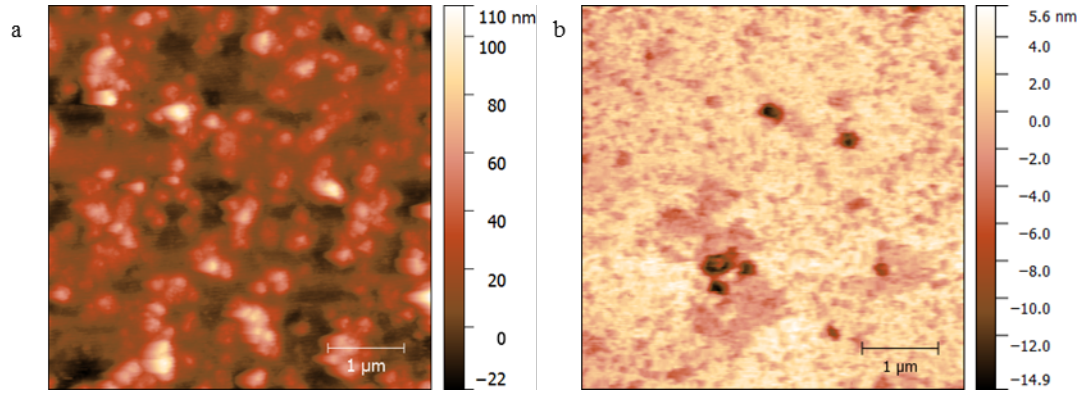

Figure 9. AFM height images of (a) L48:1 and (b) L48:4 surfaces taken in dry, ambient conditions.

DISCUSSION

Crosslinked PDMS-based films have been shown to be highly effective as AF/FR films.[25–28] The materials presented here showed facile release of sporelings of *U. linza* from the surface, in some cases exhibiting spontaneous release (i.e. without the application of shear). This excellent FR performance was superior not only to films with similar structure (i.e. having a crosslinked PDMS matrix with additives),[35,61] but also when compared to many other PDMS containing materials.[62,63] To accomplish this, the work reported here used amphiphilic PDMS-based block copolymers as additives to a crosslinked PDMS network. The block copolymers were synthesized to form a random copolymer block of a PEG containing methacrylate and a fluoroalkyl acrylate on a PDMS macroinitiator. Successful control of the ratio of these monomers and molecular weight of the final polymer permitted the synthesis of systematically varied sets of block copolymers with tailored chemical structure. Such systematic variations to provide understanding of parameters that affect performance of the films and how surface chemical properties are modified have not been previously studied for this type of material.

The films showed excellent FR performance against *U. linza,* even at low block copolymer loadings (1 and 4 wt%) in the PDMS matrix. The ability to release sporelings almost entirely (e.g., >90% removal with both M61:1 and M61:4 compared to 6% with PDMS control) from the surface with very low applied wall shear stress makes these combinations of surface-active copolymers in PDMS matrices amongst the best reported for FR of *U. linza.*[34–36] Although the release of *N. incerta* was not as marked as that for sporelings of *U. linza*, removal from L48:1 and L48:4 was approximately that of the PDMS control. The greater effectiveness of these films against *U. linza* suggests that overall they perform better against species that would be expected to adhere strongly to hydrophilic surfaces. In fact this response suggests that while the presence of a fluorocarbon in the surface-active segment is effective in directing PEG to the

surface during the coating process, it can reduce PEGs effectiveness with hydrophobic surface foulants. Further studies therefore of materials with a compositional strategy that forms a more polar surface may provide a better strategy against a broader range of foulants.

It was observed that lower molecular weight block copolymers enhanced the performance of the films to a greater extent than higher molecular weight block copolymers with similar ratios of hydrophilic and hydrophobic units. Therefore, connectivity of the monomers plays a role in producing films in which the surface properties reduce adhesion of the soft fouling organisms, likely due to increased chain mobility and ability to rearrange at the surface of lower molecular weight materials.

Additionally, the ratio of the PEGMA and AF6 monomers had a significant effect on the performance of these films. NEXAFS showed that increasing the content of AF6 co-units enriched the outer surface with fluoroalkyl side chains. The extent of this was determined by the AF6/PEGMA ratio and the molecular weight of the block copolymer. An interesting feature of the films, which appears to contribute to the performance of all compositions studied, is that after immersion in water there was enrichment of the amphiphilic block copolymer at the surface due to diffusion of PEG groups to the hydrated surface. This means that not only was PEGMA segregating to the hydrated surface, it also brought associated fluoroalkyl groups which do not move to the interface alone. Block copolymer enrichment of the film surface after water immersion enabled the hydrophilic PEGMA to partially compensate for, or offset, the effects of hydrophobic AF6 as seen by bubble contact angle measurements. Typically the surface-active block copolymer additives rendered the surfaces more hydrophilic when compared to the crosslinked PDMS control. The higher molecular weight additives had the greatest effect on the hydrophilicity of the films, especially after immersion in water for 120 h. It should be noted that

the nearly 50:50 compositions of the AF6:PEGMA at all molecular weights showed the lowest contact angle measurements for films with copolymers of a similar molecular weight. Therefore, initial composition alone does not dictate the final surface chemistry of the films, as the highest PEGMA content did not automatically lead to the most hydrophilic surface.

The fluorinated species play an important role in directing block copolymer additives to the surface during curing and have a significant effect on the surfaces even after water immersion for long time periods. This observation is important, because the films with a 50:50 to 60:40 AF6:PEGMA composition also exhibited the highest release of biomass for both species of algae. Fluoroalkyl chain species as short as AF6, have a low surface energy and are able to compete with the PDMS for surface coverage and are likely to dominate the surface when annealed in air.[33,64] These fluoroalkyl groups also orient at the surface, as observed by NEXAFS. Surface segregation of the fluorinated material has the effect of bringing additional PEGMA to the surface, making it available to be hydrated and to segregate underwater. Because the films were cured and the PDMS matrix was crosslinked, there was insufficient mobility of the fluorinated groups to allow for facile reorganization over large length scales, so it is important that the PEGMA is largely driven to the surface by the fluorinated groups prior to and during curing. After immersion in water, the effect of PEG then dominates the surface as the only hydrophilic component of the film. Balancing the AF6 content and PEGMA content of the block copolymer provides the opportunity to tune the delivery of PEG side chains to the surface. Therefore the most hydrophilic films are not the ones with the highest content of PEGMA, but those which have the correct balance between the two monomers. Since the films consisting of the lower molecular weight additives for each set of block copolymers (sets L and M) had the

highest fouling release, delivery of these block copolymers to the surface is an effective means of enhancing performance.

AFM analyses of samples L48:1 and L48:4 showed the two distinct surface morphologies exhibited by among coatings: L48:1 (the lower loading sample) had higher roughness, Fig. 9a, and L48:4 (the higher loading sample) had a smoother and mostly featureless surface. The only compositional difference between these two coatings was the amount of L48 copolymer. This trend was observed throughout all the coatings, where higher loadings produced smoother surfaces. When considered with the contact angle data, where higher loaded coatings tended to have lower contact angles, it is likely that at higher loadings the AF6:PEGMA is better able to cover the whole surface, whereas at lower loadings it is only presented as islands. There was a modest difference in roughness between the lower and higher loadings, and the surface morphology and topography did not appear to be much influenced by the copolymer molecular weight. Therefore, the biological performance essentially depended on the surface chemistry, the films with the lower molecular weight additives performing best and the films with the higher molecular weight additives performing worst, especially for fouling removal.

In a previous report two different sets of block copolymers composed of a PDMS block and either a hydrophilic PEGMA or a hydrophobic AF6 block were used separately as surface modifying additives in PDMS-based films and evaluated against two macrofouling species, *U. linza* and *Balanus amphitrite*[49] and possessed good FR properties against the sporelings and young barnacles. Thus, it appears from our current study that PEGMA and AF6 components can be added together synergistically[22,35,65] and amphiphilicity can be integrated into a multifunctional network polymer platform by the addition of tailored amphiphilic block copolymers to create a new generation of AF/FR coatings.[40]

CONCLUSIONS

Amphiphilic block copolymers consisting of PDMS segments combined with segments made from copolymers of a PEG-containing methacrylate and a fluoroalkyl acrylate were introduced into a crosslinked PDMS coating and shown to populate the coating surface by surface segregation using contact angle and NEXAFS measurements. In bioassays the coatings were evaluated using *U. linza* and *N. incerta*, species that adhere preferentially to polar and non-polar surfaces, respectively. This simple testing regimen reveals fouling characteristics sometimes overlooked by less targeted regimens. The resulting surface modified PDMS films have been shown to possess highly effective FR properties, in some cases leading to the spontaneous detachment of plants of *U. linza*. However, they are less effective against *N. incerta* suggesting that the coatings are more non-polar in character as a result of both PDMS and fluorocarbon segments. A high degree of control over film performance can be achieved by: i) varying the block copolymer content of the surface between PEG and fluorine dominated materials, and ii) varying the molecular weight of the polymer blocks. These surfaces belong to the category of amphiphilic, "ambiguous" coatings and lend further support to the effectiveness of this strategy for the creation of AF and FR materials. Films incorporating lower molecular weight block copolymers showed the best AF and FR performance in laboratory bioassays. Additionally, fine chemical tuning of the block copolymer composition improved the performance of these films. Thus, the design and molecular control of amphiphilic, surface-active block copolymers improve the capabilities of PDMS-based films for antifouling use.

AUTHOR INFORMATION

Corresponding Authors

*Christopher K. Ober, cko3@cornell.edu

Department of Materials Science and Engineering, Cornell University, Ithaca, New York 14850

*Giancarlo Galli, giancarlo.galli@unipi.it

Dipartimento di Chimica e Chimica Industriale, Università di Pisa, 56124 Pisa, Italy

Author Contributions

The manuscript was written through contributions of all authors. All authors have given approval to the final version of the manuscript.

ACKNOWLEDGMENTS

Work supported by EC Framework Programme 7 SEACOAT project (Surface Engineering for Antifouling: Coordinated Advanced Training, contract No. 237997) and the Italian MiUR (PRIN fondi 2010-2011). This work was made possible through funding from the Office of Naval Research Grant No. N000141110330 (ONR). Data presented in this publication was collected at NSLS NIST beamline U7A, which is supported by the U.S. Department of Energy, Office of Science, Office of Basic Energy Sciences under Contract No. DE-AC02-98CH10886. This work made use of the Cornell Center for Materials Research Shared Facilities which are supported through the NSF MRSEC program (DMR-1120296).

Supporting Information.

The supporting information includes AFM micrographs and surface roughness of the film surfaces showing the effect of immersion in water.

REFERENCES

(1) Callow, J. A.; Callow, M. E. Biofilms. In *Antifouling Compounds*; Fusetani, N., Clare, A. S., Eds.; Springer, 2006; pp 141–169.

(2) Schultz, M. P.; Bendick, J. A.; Holm, E. R.; Hertel, W. M. Economic Impact of Biofouling on a Naval Surface Ship. *Biofouling* **2011**, *27* (1), 87–98.

(3) Townsin, R. L. The Ship Hull Fouling Penalty. *Biofouling* **2003**, *19 Suppl* (June 2015), 9–15.

(4) Corbett, J. J. Updated Emissions from Ocean Shipping. *J. Geophys. Res.* **2003**, *108* (D20), 4650.

(5) Thomas, K. V.; Brooks, S. The Environmental Fate and Effects of Antifouling Paint Biocides. *Biofouling* **2010**, *26* (1), 73–88.

(6) Champ, M. A. Economic and Environmental Impacts on Ports and Harbors from the Convention to Ban Harmful Marine Anti-Fouling Systems. *Mar. Pollut. Bull.* **2003**, *46* (8), 935–940.

(7) Earley, P. J.; Swope, B. L.; Barbeau, K.; Bundy, R.; McDonald, J. A.; Rivera-Duarte, I. Life Cycle Contributions of Copper from Vessel Painting and Maintenance Activities. *Biofouling* **2014**, *30* (1), 51–68.

(8) Scardino, A. J.; Guenther, J.; de Nys, R. Attachment Point Theory Revisited: The Fouling Response to a Microtextured Matrix. *Biofouling* **2008**, *24* (1), 45–53.

(9) Long, C. J.; Schumacher, J. F.; Robinson, P. A. C.; Finlay, J. A.; Callow, M. E.; Callow, J.

A.; Brennan, A. B. A Model That Predicts the Attachment Behavior of *Ulva linza* Zoospores on Surface Topography. *Biofouling* **2010**, *26* (4), 411–419.

(10) Aldred, N.; Phang, I. Y.; Conlan, S. L.; Clare, A. S.; Vancso, G. J. The Effects of a Serine Protease, Alcalase, on the Adhesives of Barnacle Cyprids (*Balanus amphitrite*). *Biofouling* **2008**, *24* (2), 97–107.

(11) Tasso, M.; Pettitt, M. E.; Cordeiro, A. L.; Callow, M. E.; Callow, J. A.; Werner, C. Antifouling Potential of Subtilisin A Immobilized onto Maleic Anhydride Copolymer Thin Films. *Biofouling* **2009**, *25* (6), 505–516.

(12) Qian, P.-Y.; Li, Z.; Xu, Y.; Li, Y.; Fusetani, N. Mini-Review: Marine Natural Products and Their Synthetic Analogs as Antifouling Compounds: 2009-2014. *Biofouling* **2015**, *31* (1), 101–122.

(13) Yang, W.-J.; Neoh, K.-G.; Kang, E.-T.; Teo, S. L.-M.; Rittschof, F. Polymer brush coatings for combating marine biofouling, *Progress in Polymer Science.* **2014**, *39* 1017–1042.

(14) Jiang, S.; Cao, Z. Ultralow-Fouling, Functionalizable, and Hydrolyzable Zwitterionic Materials and Their Derivatives for Biological Applications. *Adv. Mater.* **2010**, *22* (9), 920–932.

(15) Zhang, Z.; Finlay, J. A.; Wang, L.; Gao, Y.; Callow, J. A.; Callow, M. E.; Jiang, S. Polysulfobetaine-Grafted Surfaces as Environmentally Benign Ultralow Fouling Marine Coatings. *Langmuir* **2009**, *25* (23), 13516–13521.

(16) Aldred, N.; Li, G.; Gao, Y.; Clare, A. S.; Jiang, S. Modulation of Barnacle (*Balanus amphitrite Darwi*n) Cyprid Settlement Behavior by Sulfobetaine and Carboxybetaine Methacrylate Polymer Coatings. *Biofouling* **2010**, *26* (6), 673–683.

(17) Li, X.; Andruzzi, L.; Chiellini, E.; Galli, G.; Ober, C. K.; Hexemer, A.; Kramer, E. J.; Fischer, D. A. Semifluorinated Aromatic Side-Group Polystyrene-Based Block Copolymers: Bulk Structure and Surface Orientation Studies. *Macromolecules* **2002**, *35* (21), 8078–8087.

(18) Zhang, G.; Jiang, J.; Zhang, Q.; Gao, G.; Zhan, X.; Chen, F. Ultralow Oil-Fouling Heterogeneous Poly(ether sulfone) Ultrafiltration Membrane via Blending with Novel Amphiphilic Fluorinated Gradient Copolymers *Langmuir* **2016**, *32* (5), 1380−1388.

(19) Hu, Z.; Finlay, J. A.; Chen, L.; Betts, D. E.; Hillmyer, M. A.; Callow, M. E.; Callow, J. A.; DeSimone, J. M. Photochemically Cross-Linked Perfluoropolyether-Based Elastomers: Synthesis, Physical Characterization, and Biofouling Evaluation. *Macromolecules* **2009**, *42* (18), 6999–7007.

(20) Gudipati, C. S.; Finlay, J. A.; Callow, J. A.; Callow, M. E.; Wooley, K. L. The Antifouling and Fouling-Release Perfomance of Hyperbranched Fluoropolymer (HBFP)-Poly(ethylene Glycol) (PEG) Composite Coatings Evaluated by Adsorption of Biomacromolecules and the Green Fouling Alga *Ulva*. *Langmuir* **2005**, *21* (7), 3044–3053.

(22) Martinelli, E.; Del Moro, I.; Galli, G.; Barbaglia, M.; Bibbiani, C.; Mennillo, E.; Oliva, M.; Pretti, C.; Antonioli, D.; Laus, M. Photopolymerized Network Polysiloxane Films with Dangling Hydrophilic/Hydrophobic Chains for the Biofouling Release of Invasive Marine Serpulid *Ficopomatus enigmaticus*. *ACS Appl. Mater. Interfaces* **2015**, *7* (15), 8293–8301.

(28) Andruzzi, L.; Senaratne, W.; Hexemer, A.; Sheets, E. D.; Ilic, B.; Kramer, E. J.; Baird, B.; Ober, C. K. Oligo(ethylene Glycol) Containing Polymer Brushes as Bioselective Surfaces.

Langmuir **2005**, *21* (6), 2495–2504.

(23) Ma, H.; Hyun, J.; Stiller, P.; Chilkoti, A. "Non-Fouling" Oligo(ethylene Glycol)-Functionalized Polymer Brushes Synthesized by Surface-Initiated Atom Transfer Radical Polymerization. *Adv. Mater.* **2004**, *16* (4), 338–341.

(24) Hawkins, M. L.; Faÿ, F.; Réhel, K.; Linossier, I.; Grunlan, M. A. Bacteria and Diatom Resistance of Silicones Modified with PEO-Silane Amphiphiles. *Biofouling* **2014**, *30* (2), 247–258.

(25) Brady, R. F.; Singer, I. L. Mechanical Factors Favoring Release from Fouling Release Coatings. *Biofouling* **2000**, *15* (1-3), 73–81.

(26) Kim, J.; Chisholm, B. J.; Bahr, J. Adhesion Study of Silicone Coatings: The Interaction of Thickness, Modulus and Shear Rate on Adhesion Force. *Biofouling* **2007**, *23* (1-2), 113–120.

(27) Wynne, K.; Swain, G.; Fox, R.; Bullock, S.; Uilk, J. Two Silicone Nontoxic Fouling Release Coatings: Hydrosilation Cured PDMS and CaCO3 Filled, Ethoxysiloxane Cured RTV11. *Biofouling* **2000**, *16* (2-4), 277–288.

(28) Wendt, D. E.; Kowalke, G. L.; Kim, J.; Singer, I. L. Factors That Influence Elastomeric Coating Performance: The Effect of Coating Thickness on Basal Plate Morphology, Growth and Critical Removal Stress of the Barnacle *Balanus amphitrite*. *Biofouling* **2006**, *22* (1-2), 1–9.

(29) Kavanagh, C. J.; Swain, G. W.; Kovach, B. S.; Stein, J.; Darkangelo-Wood, C.; Truby, K.; Holm, E.; Montemarano, J.; Meyer, A.; Wiebe, D. The Effects of Silicone Fluid Additives and Silicone Elastomer Matrices on Barnacle Adhesion Strength. *Biofouling* **2003**, *19* (6), 381–390.

(30) Beigbeder, A.; Degee, P.; Conlan, S. L.; Mutton, R. J.; Clare, A. S.; Pettitt, M. E.; Callow, M. E.; Callow, J. A.; Dubois, P. Preparation and Characterisation of Silicone-Based Coatings Filled with Carbon Nanotubes and Natural Sepiolite and Their Application as Marine Fouling-Release Coatings. *Biofouling* **2008**, *24* (4), 291–302.

(31) Majumdar, P.; Lee, E.; Patel, N.; Stafslien, S. J.; Daniels, J.; Chisholm, B. J. Development of Environmentally Friendly, Antifouling Coatings Based on Tethered Quaternary Ammonium Salts in a Crosslinked Polydimethylsiloxane Matrix. *J. Coat. Technol. Res.* **2008**, *5* (4), 405–417.

(32) Calabrese, D. R.; Wenning, B.; Finlay, J. A.; Callow, M. E.; Callow, J. A.; Fischer, D.; Ober, C. K. Amphiphilic Oligopeptides Grafted to PDMS-Based Diblock Copolymers for Use in Antifouling and Fouling Release Coatings. *Polym. Adv. Technol.* **2015**, *26* (7), 829–836.

(33) Martinelli, E.; Guazzelli, E.; Bartoli, C.; Gazzarri, M.; Chiellini, F.; Galli, G.; Callow, M. E.; Callow, J. A.; Finlay, J. A.; Hill, S. Amphiphilic Pentablock Copolymers and Their Blends with PDMS for Antibiofouling Coatings. *J. Polym. Sci. Part A Polym. Chem.* **2015**, *53* (10), 1213–1225.

(34) Martinelli, E.; Suffredini, M.; Galli, G.; Glisenti, A.; Pettitt, M. E.; Callow, M. E.; Callow, J. A.; Williams, D.; Lyall, G. Amphiphilic Block Copolymer/poly(dimethylsiloxane) (PDMS) Blends and Nanocomposites for Improved Fouling-Release. *Biofouling* **2011**, *27* (5), 529–541.

(35) Martinelli, E.; Sarvothaman, M. K.; Galli, G.; Pettitt, M. E.; Callow, M. E.; Callow, J. A.; Conlan, S. L.; Clare, A. S.; Sugiharto, A. B.; Davies, C.; Williams, D. Poly(dimethyl Siloxane) (PDMS) Network Blends of Amphiphilic Acrylic Copolymers with

Poly(ethylene Glycol)-Fluoroalkyl Side Chains for Fouling-Release Coatings. II. Laboratory Assays and Field Immersion Trials. *Biofouling* **2012**, *28* (6), 571–582.

(36) Yasani, B. R.; Martinelli, E.; Galli, G.; Glisenti, A.; Mieszkin, S.; Callow, M. E.; Callow, J. A. A Comparison between Different Fouling-Release Elastomer Coatings Containing Surface-Active Polymers. *Biofouling* **2014**, *30* (4), 387–399.

(37) Muthukrishnan, T.; Abed, R. M. M.; Dobretsov, S.; Kidd, B.; Finnie, A. A. Long-Term Microfouling on Commercial Biocidal Fouling Control Coatings. *Biofouling* **2014**, *30* (10), 1155–1164.

(38) Schultz, M. P.; Walker, J. M.; Steppe, C. N.; Flack, K. A. Impact of Diatomaceous Biofilms on the Frictional Drag of Fouling-Release Coatings. *Biofouling* **2015**, *31* (9-10), 759–773.

(39) Hearin, J.; Hunsucker, K. Z.; Swain, G.; Stephens, A.; Gardner, H.; Lieberman, K.; Harper, M. Analysis of Long-Term Mechanical Grooming on Large-Scale Test Panels Coated with an Antifouling and a Fouling-Release Coating. *Biofouling* **2015**, *31* (8), 625–638.

(40) Galli, G.; Martinelli, E.; Amphiphilic Polymer Platforms: Surface Engineering of Films for Marine Antibiofouling. *Macromol. Rapid Commun.* **2017**, DOI: 10.1002/marc.201600704, and references therein.

(41) Cho, Y.; Sundaram, H. S.; Weinman, C. J.; Paik, M. Y.; Dimitriou, M. D.; Finlay, J. A.; Callow, M. E.; Callow, J. A.; Kramer, E. J.; Ober, C. K. Triblock Copolymers with Grafted Fluorine-Free, Amphiphilic, Non-Ionic Side Chains for Antifouling and Fouling-Release Applications. *Macromolecules* **2011**, *44* (12), 4783–4792.

(42) Dimitriou, M. D.; Zhou, Z.; Yoo, H.-S.; Killops, K. L.; Finlay, J. A.; Cone, G.; Sundaram,

H. S.; Lynd, N. A.; Barteau, K. P.; Campos, L. M.; Fischer, D. A.; Callow, M. E.; Callow, J. A.; Ober, C. K.; Hawker, C. J.; Kramer, E. J. A General Approach to Controlling the Surface Composition of Poly(ethylene Oxide)-Based Block Copolymers for Antifouling Coatings. *Langmuir* **2011**, *27* (22), 13762–13772.

(43) Sundaram, H. S.; Cho, Y.; Dimitriou, M. D.; Finlay, J. A.; Cone, G.; Williams, S.; Handlin, D.; Gatto, J.; Callow, M. E.; Callow, J. A.; Kramer, E. J.; Ober, C. K. Fluorinated Amphiphilic Polymers and Their Blends for Fouling-Release Applications: The Benefits of a Triblock Copolymer Surface. *ACS Appl. Mater. Interfaces* **2011**, *3* (9), 3366–3374.

(44) Cho, Y.; Sundaram, H. S.; Finlay, J. A.; Dimitriou, M. D.; Callow, M. E.; Callow, J. A.; Kramer, E. J.; Ober, C. K. Reconstruction of Surfaces from Mixed Hydrocarbon and PEG Components in Water: Responsive Surfaces Aid Fouling Release. *Biomacromolecules* **2012**, *13* (6), 1864–1874.

(45) Galli, G.; Martinelli, E.; Chiellini, E.; Ober, C. K.; Glisenti, A. Low Surface Energy Characteristics of Mesophase-Forming ABC and ACB Triblock Copolymers with Fluorinated B Blocks. *Mol. Cryst. Liq. Cryst.* **2005**, *441* (1), 211–226.

(46) Martinelli, E.; Galli, G.; Glisenti, A. Surface Behavior of Modified-Polystyrene Triblock Copolymers with Different Macromolecular Architectures. *Eur. Polym. J.* **2014**, *60*, 69–78.

(47) Martinelli, E.; Pelusio, G.; Yasani, B. R.; Glisenti, A.; Galli, G. Surface Chemistry of Amphiphilic Polysiloxane/Triethyleneglycol-Modified Poly(pentafluorostyrene) Block Copolymer Films Before and After Water Immersion. *Macromol. Chem. Phys.* **2015**, *216* (21), 2086–2094.

(48) Martinelli, E.; Galli, G.; Cwikel, D.; Marmur, A. Wettability and Surface Tension of Amphiphilic Polymer Films: Time-Dependent Measurements of the Most Stable Contact Angle. *Macromol. Chem. Phys.* **2012**, *213* (14), 1448–1456.

(49) Martinelli, E.; Gunes, D.; Wenning, B. M.; Ober, C. K.; Finlay, J. A.; Callow, M. E.; Callow, J. A.; Di Fino, A.; Clare, A. S.; Galli, G. Effects of Surface-Active Block Copolymers with Oxyethylene and Fluoroalkyl Side Chains on the Antifouling Performance of Silicone-Based Films. *Biofouling* **2016**, *32* (1), 81–93.

(50) Pester, C. W.; Poelma, J. E.; Narupai, B.; Patel, S. N.; Su, G. M.; Mates, T. E.; Luo, Y.; Ober, C. K.; Hawker, C. J.; Kramer, E. J. Ambiguous Anti-Fouling Surfaces: Facile Synthesis by Light-Mediated Radical Polymerization. *J. Polym. Sci. Part A Polym. Chem.* **2016**, *54* (2), 253–262.

(51) Finlay, J. A.; Krishnan, S.; Callow, M. E.; Callow, J. A.; Dong, R.; Asgill, N.; Wong, K.; Kramer, E. J.; Ober, C. K. Settlement of Ulva Zoospores on Patterned Fluorinated and PEGylated Monolayer Surfaces. *Langmuir* **2008**, *24* (2), 503–510.

(52) Mielczarski, J. A.; Mielczarski, E.; Galli, G.; Morelli, A.; Martinelli, E.; Chiellini, E. The Surface-Segregated Nanostructure of Fluorinated Copolymer- Poly(dimethylsiloxane) Blend Films. *Langmuir* **2010**, *26* (4), 2871–2876.

(53) Andrade, J. D.; King, R. N.; Gregonis, D. E.; Coleman, D. L. Surface Characterization of Poly(hydroxyethyl Methacrylate) and Related Polymers. I. Contact Angle Methods in Water. *J. Polym. Sci. Polym. Symp.* **1979**, *66*, 313–336.

(54) Genzer, J.; Sivaniah, E.; Kramer, E. J.; Wang, J.; Körner, H.; Char, K.; Ober, C. K.; DeKoven, B. M.; Bubeck, R. A.; Fischer, D. A.; Sambasivan, S. Temperature Dependence of Molecular Orientation on the Surfaces of Semifluorinated Polymer Thin Films.

Langmuir **2000**, *16* (4), 1993–1997.

(55) Sohn, K. E.; Dimitriou, M. D.; Genzer, J.; Fischer, D. A.; Hawker, C. J.; Kramer, E. J. Determination of the Electron Escape Depth for NEXAFS Spectroscopy. *Langmuir* **2009**, *25* (11), 6341–6348.

(56) Schultz, M. P.; Finlay, J. A.; Callow, M. E.; Callow, J. A. A Turbulent Channel Flow Apparatus for the Determination of the Adhesion Strength of Microfouling Organisms. *Biofouling* **2000**, *15* (4), 243–251.

(57) Callow, M. E.; Callow, J. A.; Pickett-Heaps, J. D.; Wetherbee, R. Primary Adhesion of *Enteromorpha* (Chlorophyta, Ulvales) Propagules: Quantitative Settlement Studies and Video Microscopy. *J. Phycol.* **1997**, *33* (6), 938–947.

(58) Finlay, J. A.; Fletcher, B. R.; Callow, M. E.; Callow, J. A. Effect of Background Colour on Growth and Adhesion Strength of *Ulva* Sporelings. *Biofouling* **2008**, *24* (3), 219–225.

(59) Krishnan, S.; Wang, N.; Ober, C. K.; Finlay, J. A.; Callow, M. E.; Callow, J. A.; Hexemer, A.; Sohn, K. E.; Kramer, E. J.; Fischer, D. A. Comparison of the Fouling Release Properties of Hydrophobic Fluorinated and Hydrophilic PEGylated Block Copolymer Surfaces: Attachment Strength of the Diatom *Navicula* and the Green Alga *Ulva*. *Biomacromolecules* **2006**, *7* (5), 1449–1462.

(60) Holland, R.; Dugdale, T. M.; Wetherbee, R.; Brennan, A. B.; Finlay, J. A.; Callow, J. A.; Callow, M. E. Adhesion and Motility of Fouling Diatoms on a Silicone Elastomer. *Biofouling* **2004**, *20* (6), 323–329.

(61) Martinelli, E.; Sarvothaman, M. K.; Alderighi, M.; Galli, G.; Mielczarski, E.; Mielczarski, J. A. PDMS Network Blends of Amphiphilic Acrylic Copolymers with Poly(ethylene Glycol)-Fluoroalkyl Side Chains for Fouling-Release Coatings. I. Chemistry and Stability

of the Film Surface. *J. Polym. Sci. Part A Polym. Chem.* **2012**, *50* (13), 2677–2686.

(62) Sommer, S.; Ekin, A.; Webster, D. C.; Stafslien, S. J.; Daniels, J.; VanderWal, L. J.; Thompson, S. E. M.; Callow, M. E.; Callow, J. A. A Preliminary Study on the Properties and Fouling-Release Performance of Siloxane-Polyurethane Coatings Prepared from Poly(dimethylsiloxane) (PDMS) Macromers. *Biofouling* **2010**, *26* (8), 961–972.

(63) Chaudhury, M. K.; Finlay, J. A.; Chung, J. Y.; Callow, M. E.; Callow, J. A. The Influence of Elastic Modulus and Thickness on the Release of the Soft-Fouling Green Alga *Ulva Linza* (Syn. *Enteromorpha Linza*) from Poly(dimethylsiloxane) (PDMS) Model Networks. *Biofouling* **2005**, *21* (1), 41–48.

(64) Martinelli, E.; Agostini, S.; Galli, G.; Chiellini, E.; Glisenti, A.; Pettitt, M. E.; Callow, M. E.; Callow, J. A.; Graf, K.; Bartels, F. W. Nanostructured Films of Amphiphilic Fluorinated Block Copolymers for Fouling Release Application. *Langmuir* **2008**, *24* (22), 13138–13147.

(65) Van Zoelen, W.; Buss, H. G.; Ellebracht, N. C.; Lynd, N. A.; Fischer, D. A.; Finlay, J.; Hill, S.; Callow, M. E.; Callow, J. A.; Kramer, E. J.; Zuckermann, R. N.; Segalman, R. A. Sequence of Hydrophobic and Hydrophilic Residues in Amphiphilic Polymer Coatings Affects Surface Structure and Marine Antifouling/Fouling Release Properties. *ACS Macro Lett*. **2014**, *3* (4), 364–368.